EnM ENDOCRINOLOGY AND METABOLISM

Original Article

Endocrinol Metab 2022;37:620-629
https://doi.org/10.3803/EnM.2022.1412
pISSN 2093-596X · eISSN 2093-5978

The Effects of Irisin on the Interaction between Hepatic Stellate Cell and Macrophage in Liver Fibrosis

Dinh Vinh Do, So Young Park, Giang Thi Nguyen, Dae Hee Choi, Eun-Hee Cho

Department of Internal Medicine, Kangwon National University School of Medicine, Chuncheon, Korea

Background: Hepatic stellate cells (HSCs) are the central players interacting with multiple cell types in liver fibrosis. The crosstalk between HSCs and macrophages has recently become clearer. Irisin, an exercise-responsive myokine, was known to have a potentially protective role in liver and renal fibrosis, especially in connection with stellate cells. This study investigated the effects of irisin on the interaction between HSCs and macrophages.

Methods: Tamm-Horsfall protein-1 (THP-1) human monocytes were differentiated into macrophages, polarized into the inflammatory M1 phenotype with lipopolysaccharide. Lieming Xu-2 (LX-2) cells, human HSCs, were treated with conditioned media (CM) from M1 macrophages, with or without recombinant irisin. HSCs responses to CM from M1 macrophages were evaluated regarding activation, proliferation, wound healing, trans-well migration, contractility, and related signaling pathway.

Results: CM from M1 macrophages significantly promoted HSC proliferation, wound healing, transwell migration, and contractility, but not activation of HSCs. Irisin co-treatment attenuated these responses of HSCs to CM. However, CM and irisin treatment did not induce any changes in HSC activation. Further, irisin co-treatment alleviated CM-induced increase of phopho-protein kinase B (pAKT), matrix metalloproteinase-9 (MMP-9), and tissue inhibitor of metalloproteinases-1 (TIMP-1).

Conclusion: These findings suggested that irisin may play a protective role in the pathogenesis of liver fibrosis, especially when working in the crosstalk between HSCs and macrophages.

Keywords: Irisin; Hepatic stellate cells; Macrophages; Liver cirrhosis

INTRODUCTION

Progression of hepatic fibrosis is a response of the liver to injury such as non-alcoholic steatohepatitis, alcohol abuse, toxins, and chronic viral infection. In the liver fibrosis, there is an excessive accumulation of extracellular matrix (ECM), in which hepatic stellate cells (HSCs) are considered the primary source of collagens and other ECM components [1,2]. During liver injury, HSCs interact with neighboring cell types to become activated HSCs through the stimulation of cytokines and growth factors, such as tumor necrosis factor alpha (TNF-α), platelet-derived growth factor (PDGF), and transforming growth factor-β (TGF-β), mostly derived from macrophages [2,3].

Conventionally, hepatic macrophages can be classified as classically pro-inflammatory macrophages (M1) or activated immunoregulatory macrophages (M2). Although phenotypic expression of macrophages in the liver is much more complicated, the population of macrophages during the early phase of in-

Received: 19 January 2022, **Revised:** 30 April 2022, **Accepted:** 7 June 2022

Corresponding author: Eun-Hee Cho
Department of Internal Medicine, Kangwon National University School of Medicine, 1 Gangwondaehak-gil, Chuncheon 24341, Korea
Tel: +82-33-258-9167, **Fax:** +82-33-258-2455, **E-mail:** ehcho@kangwon.ac.kr

jury that drives HSC activation is pro-inflammatory [2,4]. These activated hepatic macrophages initiate paracrine stimulation, followed by the perpetuation of HSCs, which is characterized by proliferation, contractility, fibrogenesis, altered matrix degradation, chemotaxis, and inflammatory signaling [2,3]. Therefore, the communication between HSCs and macrophages is the key driver of hepatic fibrogenesis.

Irisin, an exercise-induced myokine derived from the proteolytic cleavage of fibronectin III domain-containing protein 5 (FNDC5), was found to enhance the browning of white adipose tissue, consequently increasing thermogenesis as well as energy expenditure [5,6]. It was shown that irisin is involved in a variety of diseases, including obesity, diabetes, non-alcoholic fatty liver disease, carcinogenesis [7,8]. Moreover, there is some evidence supporting a potential protective role of irisin in cardiac, renal, hepatic, and pancreatic fibrosis [9-15]. More specifically, previous reports on liver fibrosis showed that irisin suppressed HSC activation and reduced ECM deposition [11,15]. However, during the crosstalk of HSCs and macrophages in hepatic fibrogenesis, which is also a crucial part of the pathophysiology of the disease, the role of irisin remains unclear. Therefore, this study was aimed to investigate the effects of irisin on the interaction between HSCs and macrophages, which was based on the treatment of conditioned media (CM) from lipopolysaccharide (LPS)-induced Tamm-Horsfall protein-1 (THP-1) macrophages on HSCs.

METHODS

Materials

The reagents used in the study were obtained from the following indicated suppliers: recombinant human/murine/rat irisin from PeproTech Inc. (#100-65, Cranbury, NJ, USA); LPS and phorbol 12-myristate 13-acetate (PMA) from Sigma-Aldrich Inc. (St. Louis, MO, USA); (3-(4,5-dimethylthiazol-2-yl)-2,5-diphenyltetrazolium bromide (MTT) from BioPrince (#MT1036, Chuncheon, Korea), primary antibodies procured from Abcam Plc (Cambridge, UK): anti-α-smooth muscle actin (α-SMA; 1:1,000, ab5694), from Cell Signaling Technology, Inc. (Danvers, MA, USA): anti-protein kinase B (AKT) (1:1,000, #9272), anti-phospho-AKT (Ser473) (1:1,000, #4060), anti-extracellular signal-regulated kinase 1/2 (ERK1/2; 1:1,000, #9102), anti-phospho-ERK1/2 (Thr202/Tyr204) (1:1,000, #9101), anti-poly(ADP-ribose) polymerase (PARP; 1:1,000, #9542), anti-cleaved-PARP (Asp214) (1:1,000, #9541), from GeneTex Inc. (Irvine, CA, USA): anti-glyceraldehyde-3-phosphate dehydrogenase (GAPDH; 1:4,000, GT239), from Santa Cruz Biotechnology Inc. (Dallas, TX, USA): anti-tissue inhibitor of metalloproteinases-1 (TIMP-1) (1:1,000, sc-365905); second antibodies from Cell Signaling Technology Inc.: anti-rabbit immunoglobulin G (IgG), horseradish peroxidase (HRP)-linked (1:5,000, #7074), anti-mouse IgG, HRP-linked (1:5,000, #7076); culture media (Dulbecco's modified Eagle's medium [DMEM], Rosewell Park Memorial Institute [RPMI] 1640) from Welgene Inc. (Gyeongsan, Korea), fetal bovine serum (FBS) from Access Cell Culture (Vista, CA, USA), penicillin-streptomycin from Life Technologies (Carlsbad, CA, USA).

Cell culture

LX-2 cells were maintained in high glucose DMEM, supplemented with 100 mL/L FBS, 100,000 U/L penicillin, and 100 mg/L streptomycin at 37°C in a humidified 5% CO_2 incubator. THP-1 cells, immortalized human monocytes, were purchased from Korean Type Culture Collection (KTCC, Seoul, Korea) and were maintained in RPMI 1640 medium, supplemented with 100 mL/L FBS, 100,000 U/L penicillin, and 100 mg/L streptomycin at 37°C in a humidified 5% CO_2 incubator.

Cell treatment and conditioned medium preparation

Non-adherent monocytic THP-1 cells were seeded at a concentration of 3×10^5 cells/well in a 6-well culture plate for 24 hours. THP-1 cells were differentiated into adherent macrophages by using PMA 100 ng/mL for 24 hours. THP-1 macrophages were rested in a fresh RPMI medium for 48 hours. After that, the medium was changed to fresh RPMI with LPS 10 ng/mL for 12 hours to polarize THP-1 macrophages into the inflammatory M1 phenotype. Then, the CM was collected and was centrifuged at 12,000 ×g for 10 minutes at 4°C, then stored at –20°C for further experiments. LX-2 cells were seeded at a concentration of 3×10^5 cells/well in a 6-well culture plate for 24 hours. Then, LX-2 cells were treated with a mixture of 75% fresh DMEM and 25% CM from M1 macrophages (fresh RPMI medium was used instead of CM as the control group), with or without irisin 10 nM for 6 or 24 hours.

Proliferation assay

LX-2 cells were seeded at a concentration of 5×10^4 cells/well in a 24-well culture plate for 24 hours. The cells were then treated with the mixture of CM from M1 macrophages, with or without irisin 10 nM for 24 hours. After the treatment, LX-2 cells were incubated with fresh DMEM containing MTT 250 ng/mL for 3 hours. The reduced MTT dye was dissolved in isopropanol and then was transferred to a 96-well plate to measure

the absorbance at 570 nm by using SpectraMax 190 Microplate Reader (Molecular Devices LLC., San Jose, CA, USA).

Migration assays

Wound healing migration assay

LX-2 cells were seeded at a concentration of 5×10^5 cells/well in a 6-well culture plate for 24 hours. When the confluence reached >90%, the cells were incubated with 1 μg/mL mitomycin C diluted in serum-free DMEM for 1 hour. Then, an injury line was made using a yellow tip, and the cell monolayer was washed twice with DMEM. The cells were subsequently incubated for 6 hours with the mixture of CM from M1 macrophages, with or without irisin 10 nM. Cell migration was observed and pictures of the injury line at 0 and 6 hours were taken via microscopy. The covered area was measured by using ImageJ version 1.8.0_112 64bit (U.S. National Institutes of Health, Bethesda, MD, USA) and was considered as representing the capability of cell migration.

Transwell migration assay

Transwell migration assay was performed using Transwell Permeable Supports (8.0 μm pore size, #3422, Corning, NY, USA) in a 24-well plate. The lower chambers of the plate wells were filled with the mixture of CM from M1 macrophages. Then, LX-2 cells (3×10^4 cells/insert) in 100 μL DMEM were plated into a transwell insert containing irisin 0 or 10 nM, followed by adding the transwell insert into the plate well and incubating for 6 hours. Subsequently, the migrated cells were fixed and stained with hematoxylin and eosin (H&E), and the migrated cells within nine separate fields of the membrane were counted under light microscopy at 200× magnification.

Cell contraction assay

The Collagen-based Contraction Assay Kit (#CBA-201, Cell Biolabs Inc., San Diego, CA, USA) was used to assess the contraction of LX-2 cells. The collagen lattice was created by mixing two parts of LX-2 cell suspension (1×10^6 cells/mL) and eight parts of cold collagen gel working solution. Following this, 0.5 mL of the cell-collagen mixture was distributed into a 24-well culture plate and was incubated at 37°C for 1 hour for complete collagen polymerization before adding 1 mL of culture medium over each gel layer. The stressed matrix was developed for 24 hours by keeping the cells in an incubator. The medium was replaced with the mixture of CM from M1 macrophages, with or without irisin 10 nM. Then, the collagen gels were gently released from the sides of the culture plate to start the contraction. Pictures of the gels were taken and the difference of the perimeters of these gels at 0 and 48 hours was measured by using ImageJ to represent the capability of cell contraction.

Western blotting

The proteins of cell lysates were separated using sodium dodecyl sulfate-polyacrylamide gel electrophoresis (SDS-PAGE) before being transferred to a polyvinylidene fluoride membrane (Millipore, Bedford, MA, USA). These membranes were blocked for 1 hour at room temperature with 5% non-fat dry milk in 1X Tris-buffered saline containing 0.5% Tween-20 (TBS-T), washed with TBS-T, then incubated with primary antibodies at 4°C overnight or for 48 hours. The membranes were then washed with TBS-T and were incubated with the appropriate horseradish peroxidase-conjugated secondary antibodies at room temperature for 80 minutes. Subsequently, the blot images were taken using ChemiDoc Imaging System (Bio-Rad Laboratories Inc., Hercules, CA, USA).

Quantitative reverse transcription-polymerase chain reaction

Total RNA was extracted with AccuPrep Universal RNA Extraction Kit (Bioneer Corp., Daejeon, Korea), and then transcribed to cDNA with Maxime RT PreMix Kit (iNtRON Biotechnology Inc., Seongnam, Korea), according to the manufacturer's instruction. Real-time polymerase chain reaction (PCR) analysis was performed by using Power SYBR Green PCR Master Mix (Life Technologies Ltd., Paisley, UK) on QuantStudio 6 Flex Real-Time PCR System (Life Technologies Holdings Pte Ltd, Singapore) with the primer sequences. The comparative C_t ($\Delta\Delta C_t$) method was used to evaluate the mRNA expressions of target genes with the C_t values of target genes normalized to GAPDH as the reference gene.

Statistical analyses

Data were presented as mean±standard error of the mean of three or more independent experiments. Differences between the treatment groups were evaluated using the Student's *t* test with Microsoft Excel for Microsoft 365 MSO version 2109 Build 16.0.14430.20292 (Redmond, WA, USA) 64-bit. Differences were considered significant when $P<0.05$.

RESULTS

Effects of CM and irisin treatment on HSCs activation

The treatment of CM from M1 macrophages did not change the

level of α-SMA regardless of irisin treatment for 6 hours (mRNA) or 24 hours (protein) (Fig. 1).

Effects of CM and irisin treatment on HSCs proliferation and contractility

LX-2 proliferation was enhanced by the treatment of CM from the M1 phenotype for 24 hours, which was attenuated by irisin 10 nM (Fig. 2A) in the MTT assay. In the gel contractility assay, CM from M1 macrophages significantly enhanced the contractility of LX-2 cells after 48 hours of treatment, which was reversed by irisin co-treatment (Fig. 2B, C).

Effects of CM and irisin treatment on HSCs migration

Migration of LX-2 cells were increased by the treatment of CM from M1 macrophages for 6 hours and was alleviated by co-treatment with irisin 10 nM in both wound healing migration (Fig. 3A-C) and transwell migration (Fig. 3B-D).

Effects of CM and irisin treatment on the signaling pathway of hepatic stellate cells

The effect of irisin on the proliferation of LX-2 could be only related to a decrease in phosphorylation of AKT (Fig. 4A, B). Protein expression of TIMP-1 was enhanced with a 6-hour treatment of CM from M1 macrophages and was attenuated by co-treatment with irisin 10 nM (Fig. 4A-C). This treatment for 6 hours increased the mRNA expressions of TIMP-1, matrix metalloproteinase-9 (MMP-9), but decreased in matrix metalloproteinase-2 (MMP-2). In addition, co-treatment with irisin 10 nM reduced the expressions of TIMP-1 and MMP-9 but had no effect on MMP-2 (Fig. 4D).

Effects of CM and irisin treatment on M1 polarization of macrophages

We checked the effect of irsin on macrophage polarization. THP-1 M0 macrophages were polarized into M1 phenotype and

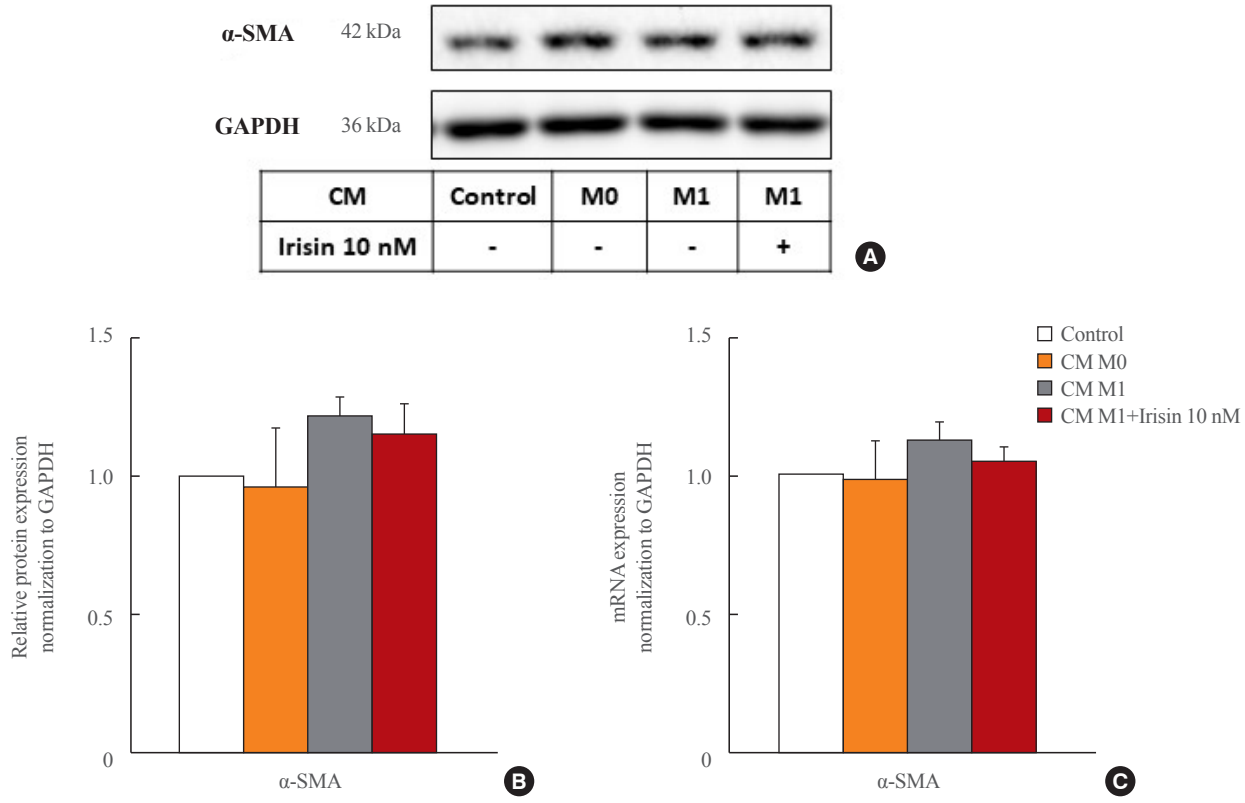

Fig. 1. Effects of conditioned media (CM) and irisin treatment on hepatic stellate cell activation. LX-2 cells were treated with CM from M1 macrophages with or without irisin 10 nM for 6 or 24 hours. M0 control (lipopolysaccharide-untreated CM). (A, B) Western blotting analysis of the protein expressions of α-smooth muscle actin (α-SMA) and glyceraldehyde-3-phosphate dehydrogenase (GAPDH) in LX-2 cells after 24 hours treatment. Representative Western blot images (A) and relative densitometric analysis (B) of three independent experiments with protein expression normalized to GAPDH. (C) Real-time polymerase chain reaction analysis of relative mRNA expression of α-SMA normalized to GAPDH in LX-2 cells after 6 hours treatment. All data are presented as mean±standard error of the mean (n=3).

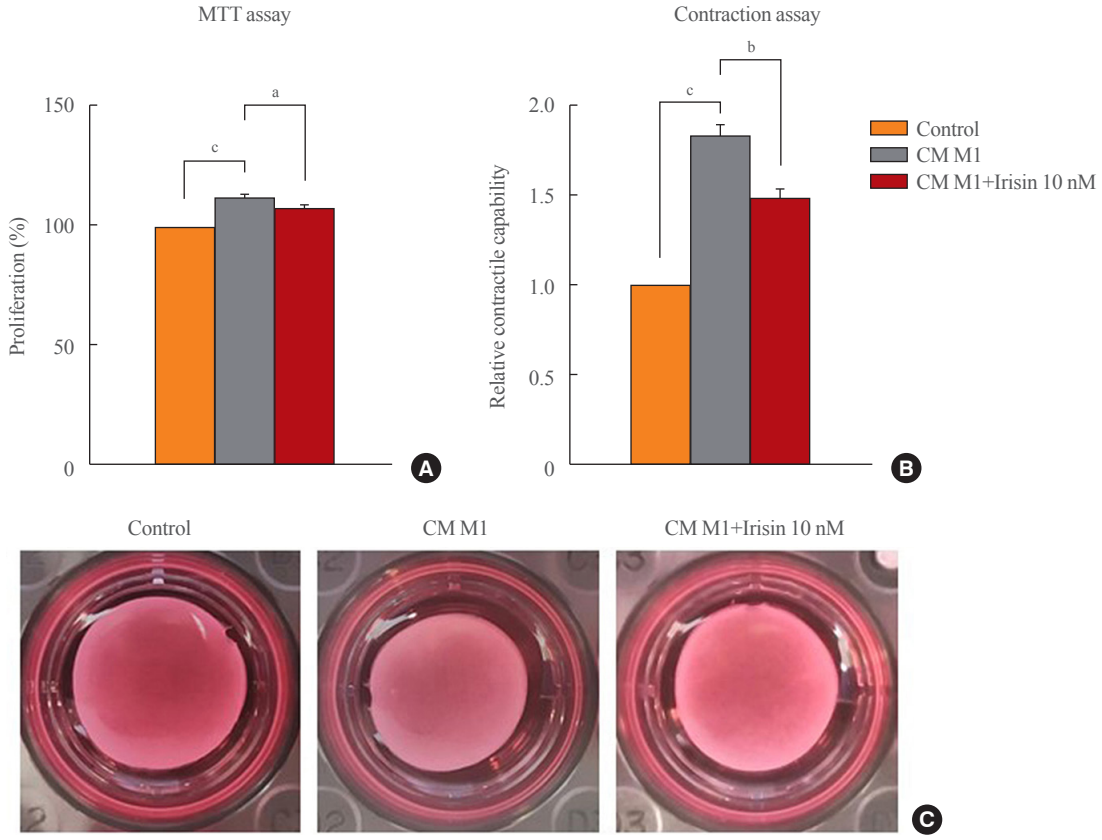

Fig. 2. Effects of conditioned media (CM) and irisin treatment on hepatic stellate cell proliferation and contractility. (A) LX-2 cells were treated with CM from M1 macrophages with or without irisin 10 nM for 24 hours and (3-(4,5-dimethylthiazol-2-yl)-2,5-diphenyltetrazolium bromide (MTT) assay was used to evaluate LX-2 cells proliferation. (B, C) Cell contraction assay was used to evaluate LX-2 cells contractile capability with the treatment of CM from M1 macrophages with or without irisin 10 nM for 48 hours. Relative contractile capability analysis by measuring the perimeter difference of gels at 0 and 48 hours (B) and representative images of cell contraction assays (C) from three independent experiments. All data are presented as mean±standard error of the mean ($n=3$). $^{a}P<0.05$; $^{b}P<0.01$; $^{c}P<0.001$.

treated with different concentration of irisin (10, 25, 50 nM). When irisin was treated during polarization into M1 phenotype, there was no difference in the expression of interleukin-1β and TNF-α (M1 markers). Therefore, irisin did not affect M1 polarization of macrophages (Fig. 5).

DISCUSSION

The findings of this study showed that CM from M1 macrophages could induce perpetuation of HSCs and that recombinant irisin effectively attenuated fibrotic response of HSCs to CM, implying a beneficial role of myokine irisin in liver fibrosis.

Liver fibrosis is a multifactorial and progressive condition in which HSCs are known as the key players. In the complex environment of the liver, HSCs interact with multiple cell types, of which macrophages (Kupffer cells and monocytederived macrophages) are predominant and are considered as important determinants in both the progression and resolution of liver fibrosis [1-3]. It was reported that macrophage depletion during liver injury attenuated fibrogenesis, while depletion during recovery diminished regression of fibrosis [16,17]. Hepatic macrophages get involved during liver fibrosis in several ways, such as regulation of inflammatory, fibrogenic cytokines, and chemokines, as well as MMPs, recruitment and infiltration of immune cells, and apoptosis of HSCs [2,3,18]. Immune modulation targeting hepatic macrophages has recently been considered a promising antifibrotic strategy [18,19].

The health benefits of exercise are well-known and the role of irisin in various conditions and diseases has been progressively explored [7,8]. Concerning macrophages, several studies reported that the inflammatory status of LPS-activated macrophages was attenuated after treatment with exogenous irisin

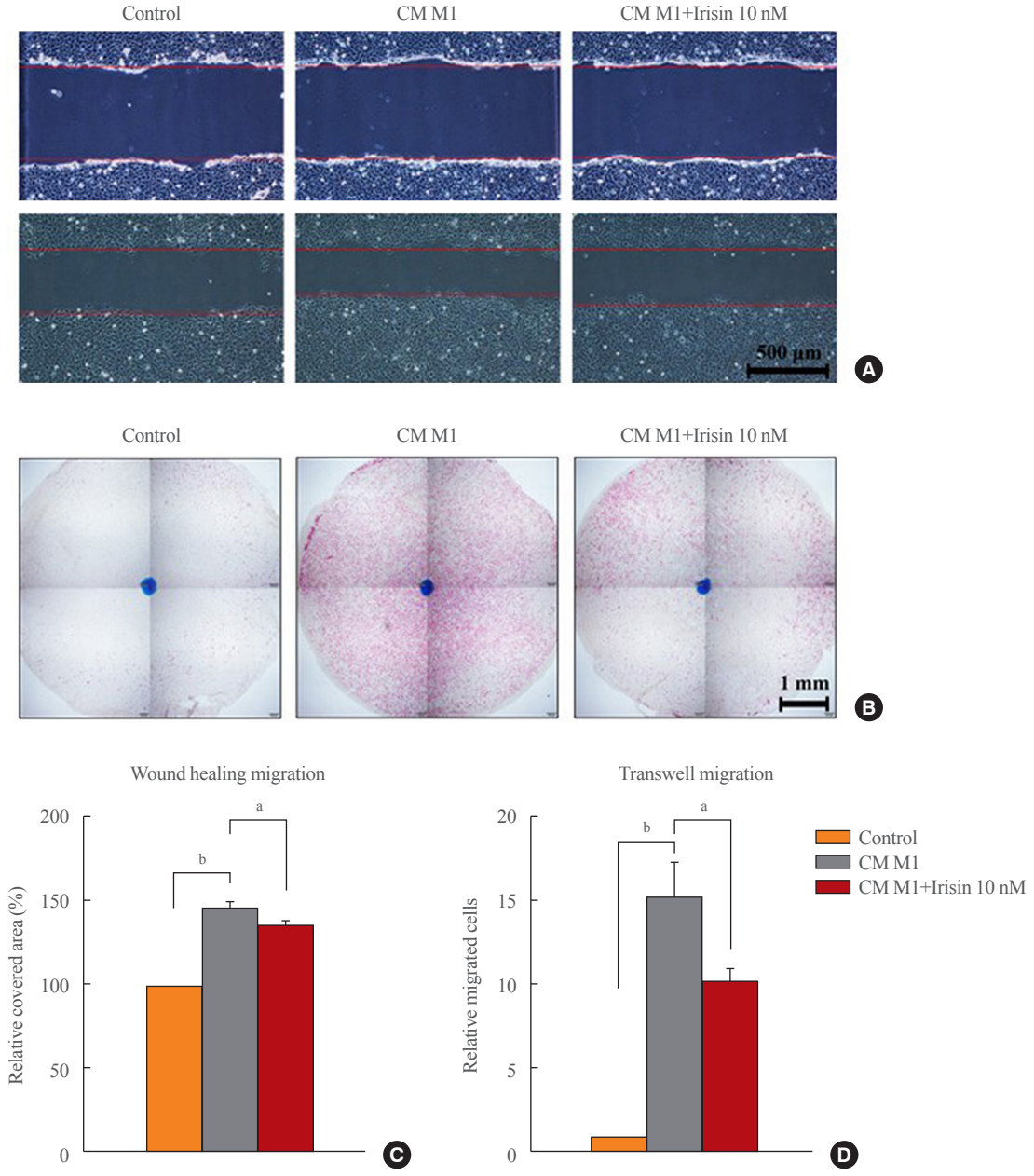

Fig. 3. Effects of conditioned media (CM) and irisin treatment on hepatic stellate cell migration. (A, B) LX-2 cells were treated with CM from M1 macrophages with or without irisin 10 nM for 6 hours to evaluate cell migration. Representative images of wound healing migration (×40) (A) and transwell migration (×40) (B) from three independent experiments. (C, D) Statistical analyses of wound healing migration (C) shown as relative covered area and transwell migration (D) shown as relative migrated cells. All data are presented as mean±standard error of the mean (n=3). [a]P<0.05; [b]P<0.001.

[20-22]. Additionally, our confirmation showed that irisin suppressed the release of pro-inflammatory cytokines and inhibited the oxidative stress in LPS-induced macrophages (Supplemental Fig. S1). The beneficial role of irisin has also been documented based on the treatment of HSCs as mentioned earlier [11,15]. Considering the potential protective role of irisin in such a complex setting of liver fibrosis, we assessed the effects of irisin on the close relationship between HSCs and macrophages based on LX-2 treatment with CM of pro-inflammatory THP-1 macrophages. Previous studies using a co-culture or CM-treatment model have shown that activated macrophages induced activation of HSCs and that molecular mechanisms re-

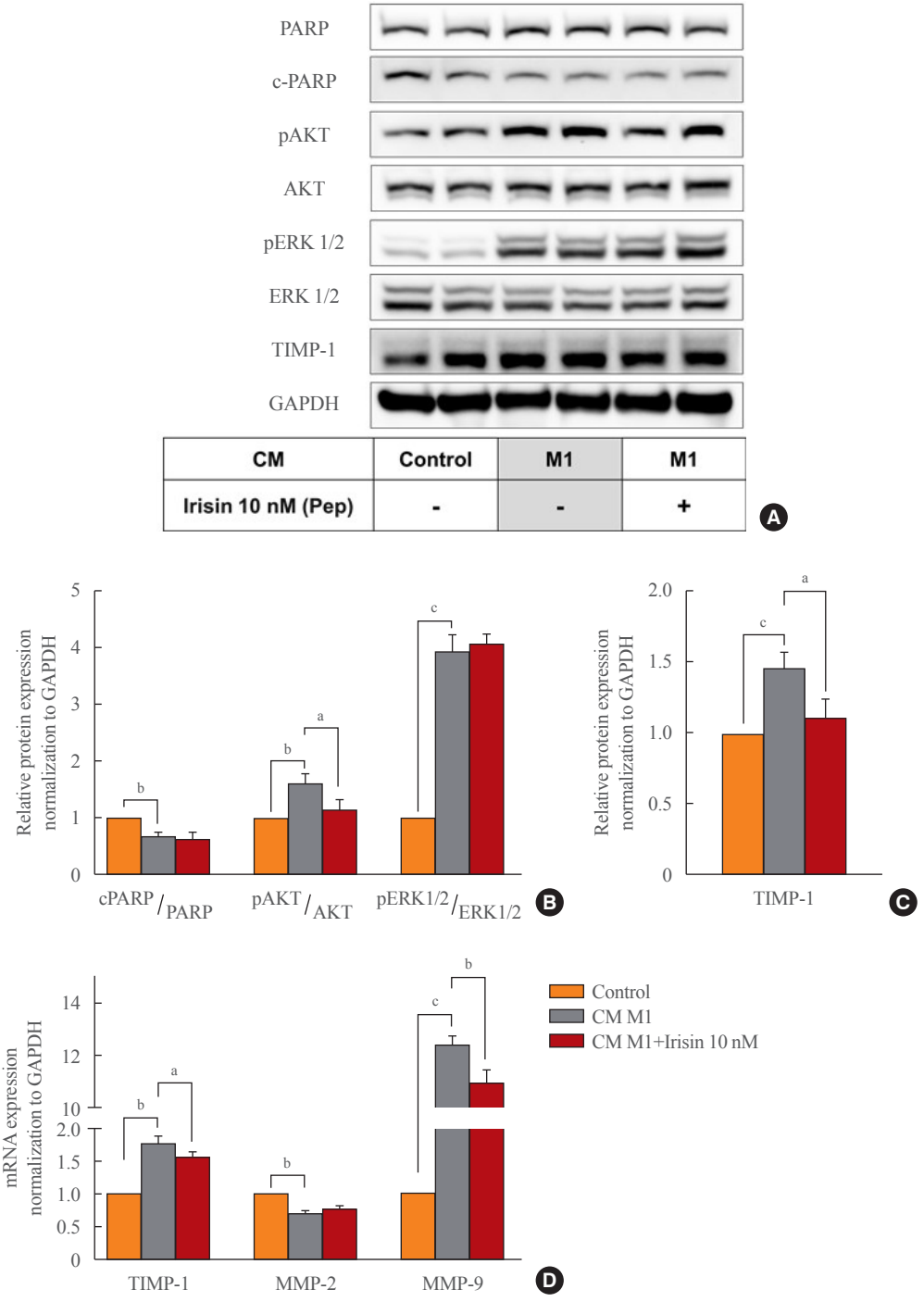

Fig. 4. Effects of conditioned media (CM) and irisin treatment on the signaling pathway of hepatic stellate cells. LX-2 cells were treated with CM from M1 macrophages with or without irisin 10 nM for 6 hours. (A-C) Western blotting analysis of the protein expressions of poly (ADP-ribose) polymerase (PARP), cleaved-PARP (c-PARP), phopho-protein kinase B (pAKT), AKT, phospho-extracellular signal-regulated kinase 1/2 (pERK1/2), ERK1/2, and glyceraldehyde-3-phosphate dehydrogenase (GAPDH) in LX-2 cells after 6 hours treatment. Representative Western blot images (A) and relative densitometric analysis of PARP, c-PARP, pAKT, AKT, pERK1/2, ERK1/2 (B) and of tissue inhibitor of metalloproteinase 1 (TIMP-1) (C) of three independent experiments with protein expression normalized to GAPDH. (D) Real-time polymerase chain reaction analysis of relative mRNA expression of TIMP-1, matrix metalloproteinase-2 (MMP-2), matrix metalloproteinase-9 (MMP-9) normalized to GAPDH in LX-2 cells after 6 hours treatment. All data are presented as mean±standard error of the mean (n=3). $^{a}P<0.05$; $^{b}P<0.01$; $^{c}P<0.001$.

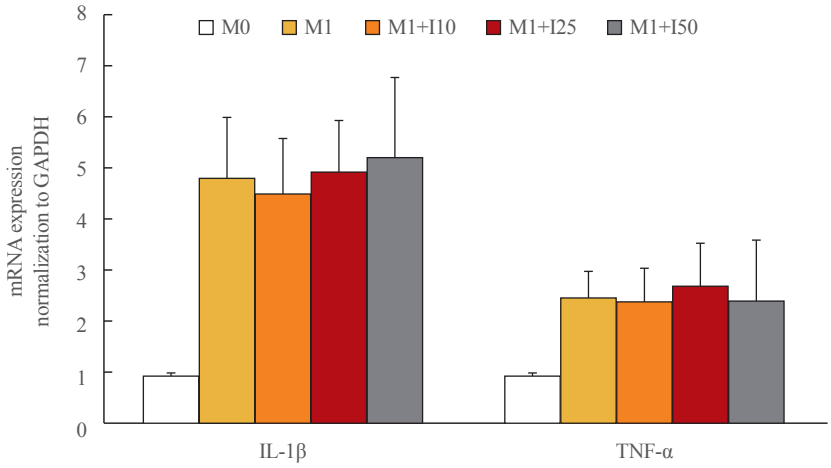

Fig. 5. Effects of conditioned media and irisin treatment on M1 polarization. Tamm-Horsfall protein-1 (THP-1) M0 macrophages were polarized into M1 phenotype and treated with different concentration of irisin (10, 25, 50 nM). All data are presented as mean±standard error of the mean (n=3). GAPDH, glyceraldehyde-3-phosphate dehydrogenase; IL-1β, interleukin-1β; TNF-α, tumor necrosis factor alpha.

lated to this communication have been increasingly investigated [17,23-26]. Herein, although CM from M1 macrophages did not induce fibrogenesis of HSCs, we observed a significant change in other properties of HSC perpetuation, including increased proliferation, migration, and contractility. In addition, treatment of recombinant irisin reduced these responses of HSCs to CM from M1 macrophages, suggesting that irisin could inhibit the activation of HSCs stimulated by macrophages.

Activation of PDGF signaling triggers several downstream pathways, such as phospholipase Cγ, phosphatidylinositol 3-kinase (PI3K)/AKT, the signal transducer and activator of transcription (STAT) and TGF-β that induces downstream SMAD proteins, and some mitogen-activated protein kinase (MAPK) pathways, such as ERK, p38, and c-jun N-terminal kinase (JNK). Regulation of these downstream signaling pathways results in proliferation, migration, fibrogenesis, and survival of HSCs [2,3,27,28]. Moreover, previous studies reported that irisin showed its effects mostly through regulating the downstream signaling pathway of MAPK. Irisin was also demonstrated to be a regulator in AMPK, PI3K/AKT, and STAT3/Snail signaling [29]. Specifically, irisin inhibited proliferation, migration, and invasion, as well as induced apoptosis in cancer cells by inhibiting the PI3K/AKT pathway or stimulating PARP cleavage [30]. Irisin increased the proliferation of human umbilical vein endothelial cells by promoting the ERK1/2 pathway [31]. Our findings showed that CM from M1 macrophages suppressed apoptosis of HSCs by inhibiting PARP cleavage, and increased proliferation and migration of HSCs by activating the AKT and ERK1/2 pathways. Additionally, irisin co-treatment reversed these effects by inhibiting only the AKT signaling pathway.

Besides chemoattractant molecules, early ECM degradation is the key element for activated HSC migration to injured sites, followed by ECM remodeling, in which MMPs and TIMPs are key drivers [3,4]. HSCs are the important source of TIMP-1 and TIMP-2; an increase in these inhibitors is associated with progressive fibrosis [32]. The expression of MMPs, particularly MMP-2 and MMP-9, is considered the key event to alter ECM and facilitate HSC migration [32,33]. The elevation of TIMP-1, MMP-2, MMP-9 in this study could be related to the increases in HSC migration induced by the CM from inflammatory macrophages. We also found that irisin co-treatment diminished HSCs migration and MMP-9, TIMP-1 expression, suggesting irisin acts through regulation of MMP-9 and TIMP-1.

Several human studies have shown the beneficial effect of exercise in patients with cirrhosis. In most studies, this benefit was demonstrated as an improvement in VO_2 max or improvement in endurance as measured by the 6-minute walk test [34]. Future studies are needed to establish the safe and effective exercise regimens in patients with cirrhosis and research into the role of muscle function in liver cirrhosis remains limited by an ongoing poor understanding of its relationship with muscle function, myokines such as irisin and liver fibrosis

In the future, further confirmation and investigation into irisin receptors are needed to further elucidate the detailed molecular mechanism of irisin effects on liver fibrosis. Interestingly, a proposed receptor of irisin, αV integrin receptor, is one of the downstream pathways of TGF-β signaling [8,35].

In conclusion, irisin was found to suppress the perpetuation

stage of HSC activation, particularly regarding HSC communication with macrophages. This supported evidence that irisin may have a favorable role in the reversal of liver fibrosis.

CONFLICTS OF INTEREST

No potential conflict of interest relevant to this article was reported.

ACKNOWLEDGMENTS

This research was supported by a research grant from Kangwon National University in 2018.

This article is based on author Dinh Vinh Do's Master's thesis: Dinh Vinh Do (2022). The effects of irisin on the interaction between hepatic stellate cell and macrophage (Masteral dissertation, Kangwon National University, Chuncheon, Korea). This work was presented as a poster oral presentation in SICEM 2021 with the title of 'The effects of irisin on the interaction between LX-2 hepatic stellate cell and THP-1 macrophage.'

AUTHOR CONTRIBUTIONS

Conception or design: D.H.C., E.H.C. Acquisition, analysis, or interpretation of data: D.V.D., S.Y.P., G.T.N. Drafting the work or revising: D.V.D. Final approval of the manuscript: D.H.C., E.H.C.

ORCID

Dinh Vinh Do *https://orcid.org/0000-0002-2280-1031*
Eun-Hee Cho *https://orcid.org/0000-0002-1349-8894*

REFERENCES

1. Hernandez-Gea V, Friedman SL. Pathogenesis of liver fibrosis. Annu Rev Pathol 2011;6:425-56.
2. Roehlen N, Crouchet E, Baumert TF. Liver fibrosis: mechanistic concepts and therapeutic perspectives. Cells 2020;9:875.
3. Tsuchida T, Friedman SL. Mechanisms of hepatic stellate cell activation. Nat Rev Gastroenterol Hepatol 2017;14:397-411.
4. Schuppan D, Surabattula R, Wang XY. Determinants of fibrosis progression and regression in NASH. J Hepatol 2018;68:238-50.
5. Bostrom P, Wu J, Jedrychowski MP, Korde A, Ye L, Lo JC, et al. A PGC1-α-dependent myokine that drives brown-fat-like development of white fat and thermogenesis. Nature 2012;481:463-8.
6. Huh JY, Panagiotou G, Mougios V, Brinkoetter M, Vamvini MT, Schneider BE, et al. FNDC5 and irisin in humans: I. Predictors of circulating concentrations in serum and plasma and II. mRNA expression and circulating concentrations in response to weight loss and exercise. Metabolism 2012;61:1725-38.
7. Korta P, Pochec E, Mazur-Bialy A. Irisin as a multifunctional protein: implications for health and certain diseases. Medicina (Kaunas) 2019;55:485.
8. Maak S, Norheim F, Drevon CA, Erickson HP. Progress and challenges in the biology of FNDC5 and irisin. Endocr Rev 2021;42:436-56.
9. Peng H, Wang Q, Lou T, Qin J, Jung S, Shetty V, et al. Myokine mediated muscle-kidney crosstalk suppresses metabolic reprogramming and fibrosis in damaged kidneys. Nat Commun 2017;8:1493.
10. Petta S, Valenti L, Svegliati-Baroni G, Ruscica M, Pipitone RM, Dongiovanni P, et al. Fibronectin type III domain-containing protein 5 rs3480 A>G polymorphism, irisin, and liver fibrosis in patients with nonalcoholic fatty liver disease. J Clin Endocrinol Metab 2017;102:2660-9.
11. Zhou B, Ling L, Zhang F, Liu TY, Zhou H, Qi XH, et al. Fibronectin type III domain-containing 5 attenuates liver fibrosis via inhibition of hepatic stellate cell activation. Cell Physiol Biochem 2018;48:227-36.
12. Chen RR, Fan XH, Chen G, Zeng GW, Xue YG, Liu XT, et al. Irisin attenuates angiotensin II-induced cardiac fibrosis via Nrf2 mediated inhibition of ROS/TGFβ1/Smad2/3 signaling axis. Chem Biol Interact 2019;302:11-21.
13. Liao Q, Qu S, Tang LX, Li LP, He DF, Zeng CY, et al. Irisin exerts a therapeutic effect against myocardial infarction via promoting angiogenesis. Acta Pharmacol Sin 2019;40:1314-21.
14. Ren Y, Zhang J, Wang M, Bi J, Wang T, Qiu M, et al. Identification of irisin as a therapeutic agent that inhibits oxidative stress and fibrosis in a murine model of chronic pancreatitis. Biomed Pharmacother 2020;126:110101.
15. Dong HN, Park SY, Le CT, Choi DH, Cho EH. Irisin regulates the functions of hepatic stellate cells. Endocrinol Metab (Seoul) 2020;35:647-55.
16. Duffield JS, Forbes SJ, Constandinou CM, Clay S, Partolina M, Vuthoori S, et al. Selective depletion of macrophages re-

veals distinct, opposing roles during liver injury and repair. J Clin Invest 2005;115:56-65.
17. Han J, Zhang X, Lau JK, Fu K, Lau HC, Xu W, et al. Bone marrow-derived macrophage contributes to fibrosing steatohepatitis through activating hepatic stellate cells. J Pathol 2019;248:488-500.
18. Cheng D, Chai J, Wang H, Fu L, Peng S, Ni X. Hepatic macrophages: key players in the development and progression of liver fibrosis. Liver Int 2021;41:2279-94.
19. Tacke F. Targeting hepatic macrophages to treat liver diseases. J Hepatol 2017;66:1300-12.
20. Mazur-Bialy AI, Pochec E, Zarawski M. Anti-inflammatory properties of irisin, mediator of physical activity, are connected with TLR4/MyD88 signaling pathway activation. Int J Mol Sci 2017;18:701.
21. Mazur-Bialy AI, Pochec E. The time-course of antioxidant irisin activity: role of the Nrf2/HO-1/HMGB1 axis. Antioxidants (Basel) 2021;10:88.
22. Li Q, Tan Y, Chen S, Xiao X, Zhang M, Wu Q, et al. Irisin alleviates LPS-induced liver injury and inflammation through inhibition of NLRP3 inflammasome and NF-κB signaling. J Recept Signal Transduct Res 2021;41:294-303.
23. Naim A, Baig MS. Matrix metalloproteinase-8 (MMP-8) regulates the activation of hepatic stellate cells (HSCs) through the ERK-mediated pathway. Mol Cell Biochem 2020;467:107-16.
24. Chen L, Yao X, Yao H, Ji Q, Ding G, Liu X. Exosomal miR-103-3p from LPS-activated THP-1 macrophage contributes to the activation of hepatic stellate cells. FASEB J 2020;34:5178-92.
25. Robert S, Gicquel T, Bodin A, Fautrel A, Barreto E, Victoni T, et al. Influence of inflammasome pathway activation in macrophages on the matrix metalloproteinase expression of human hepatic stellate cells. Int Immunopharmacol 2019;72:12-20.
26. Hu M, Wang Y, Liu Z, Yu Z, Guan K, Liu M, et al. Hepatic macrophages act as a central hub for relaxin-mediated alleviation of liver fibrosis. Nat Nanotechnol 2021;16:466-77.
27. Ying HZ, Chen Q, Zhang WY, Zhang HH, Ma Y, Zhang SZ, et al. PDGF signaling pathway in hepatic fibrosis pathogenesis and therapeutics (Review). Mol Med Rep 2017;16:7879-89.
28. Dewidar B, Meyer C, Dooley S, Meindl-Beinker AN. TGF-β in hepatic stellate cell activation and liver fibrogenesis: updated 2019. Cells 2019;8:1419.
29. Rabiee F, Lachinani L, Ghaedi S, Nasr-Esfahani MH, Megraw TL, Ghaedi K. New insights into the cellular activities of Fndc5/Irisin and its signaling pathways. Cell Biosci 2020;10:51.
30. Tsiani E, Tsakiridis N, Kouvelioti R, Jaglanian A, Klentrou P. Current evidence of the role of the myokine irisin in cancer. Cancers (Basel) 2021;13:2628.
31. Song H, Wu F, Zhang Y, Zhang Y, Wang F, Jiang M, et al. Irisin promotes human umbilical vein endothelial cell proliferation through the ERK signaling pathway and partly suppresses high glucose-induced apoptosis. PLoS One 2014;9:e110273.
32. Hemmann S, Graf J, Roderfeld M, Roeb E. Expression of MMPs and TIMPs in liver fibrosis: a systematic review with special emphasis on anti-fibrotic strategies. J Hepatol 2007;46:955-75.
33. Gong J, Han J, He J, Liu J, Han P, Wang Y, et al. Paired related homeobox protein 1 regulates PDGF-induced chemotaxis of hepatic stellate cells in liver fibrosis. Lab Invest 2017;97:1020-32.
34. Locklear CT, Golabi P, Gerber L, Younossi ZM. Exercise as an intervention for patients with end-stage liver disease: systematic review. Medicine (Baltimore) 2018;97:e12774.
35. Kisseleva T, Brenner D. Molecular and cellular mechanisms of liver fibrosis and its regression. Nat Rev Gastroenterol Hepatol 2021;18:151-66.